The Fermi Motion and J/ψ Production at the Hadron Colliders

M.A. Gomshi Nobary, B. Nikoobakht
Department of Physics, Faculty of Science, Razi University, Kermanshah, Iran.

The Fermi motion effect in J/ψ production in various hadron colliders is studied. We deduce that in agreement with sum rules which the fragmentation functions should satisfy, while the effect has considerable influence on the fragmentation probabilities and the differential cross sections, the total cross sections are essentially left unchanged.

I. INTRODUCTION

The J/ψ state has been one of the interesting problems of QCD both in theory [1,2,3] and in experiment [4]. QCD predictions for production cross section of J/ψ fails to agree with the experimental results. Color octet senario is introduced to bring about the agreement [5,6].

In this work, we introduce the Fermi motion into the J/ψ production. We only include the charm fragmentation contributions. The Tevatron Run I, the Tevatron Run II, the RHIC and the CERN LHC energies are considered to demonstrate the effect.

II. FRAGMENTATION FUNCTIONS

With the choice of a light cone the wave function, we introduce the Fermi motion effect in fragmentation production of the J/ψ bound state. In the leading order perturbative regime, the fragmentation functions for J/ψ production without and with the Fermi motion are obtained [7].

In the absence of Fermi motion, where the confinement parameter is $\beta = 0$, the fragmentation function has the following form

$$D_{c\to J/\psi}(z,\mu_\circ,\beta=0) = \frac{\alpha_s^2 C_F^2 \langle {k_T}^2\rangle^{1/2}}{16mF(z)}\Big\{z(1-z)^2\Big[\xi^2z^4+2\xi z^2(4-4z+5z^2) + (16-32z+24z^2-8z^3+9z^4)\Big]\Big\}, \tag{1}$$

where α_s is the strong interaction coupling constant and C_F is the color factor. The quantity $\langle {k_T}^2\rangle$ is the average transverse momentum squared of the initial state heavy quark, the parameter ξ is defined as $\xi = \langle {k_T}^2\rangle/m^2$ and finally $F(x)$ is given by

$$F(z) = \Big[\xi^2z^4 - (z-2)^2(3z-4) + \xi z^2(8-7z+z^2)\Big]^2. \tag{2}$$

In the presence of Fermi motion the fragmentation function is obtained as

$$\begin{aligned} D_{c\to J/\psi}(z,\mu_\circ,\beta) = &\frac{\pi^2\alpha_s^2C_F^2\langle {k_T}^2\rangle^{1/2}}{2m}\int \frac{dqdx|\psi_M|^2x^2(1-z)^2zq}{G(z)} \\ &\times\Big\{1-4(1-x)z+2(4-10x+7x^2)z^2 \\ &+4(-1+x^3-5x^2+4x)z^3+(1-4x+8x^2-4x^3+x^4)z^4 \\ &+\eta\xi z^2\big[1-2x+z^2+x^2(2-2z+z^2)\big]+\eta\big[2+(-6+4x)z \end{aligned}$$

$$+(9-8x+2x^2)z^2-2(2-x+x^2)z^3+(1+x^2)z^4\big]$$
$$+\xi z^2\big[1+2x^3(2-3z)z+z^2+2x^4z^2+2x(-1+z-2z^2)$$
$$+x^2(2-8z+9z^2)\big]+\eta^2(1-z)^2+\xi^2(1-x)^2x^2z^4\Big\}. \quad (3)$$

The function $G(z)$ reads as

$$G(z) = \Big\{\big[\eta(1-z)^2+\xi x^2z^2+(1-(1-x)z)^2\big]\big[\eta(-1+z)+\xi(-1+x)xz^2-1+(1-x+x^2)z\big]\Big\}^2. \quad (4)$$

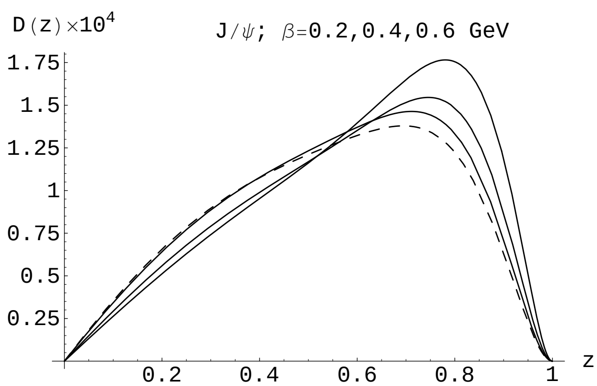

FIG. 1: Fragmentation function for J/ψ production. While the dashed curve represents the function when the Fermi motion is off, the solid ones show the behavior of this function when the Fermi motion is on. The β values are indicated. The function picks up as β increases. This gives raise to increase in the fragmentation probability.

Moreover here we have defined $\eta = q^2/m^2$.

The two cases of the Fermi motion off and on may be compared using the above fragmentation functions. Note that $\beta = 0$ and $\beta \neq 0$ correspond to these cases. For β value, we have chosen the range of β =0.0 - 0.6 GeV . The behavior of the fragmentation function (3) is shown in Fig. 1 for $\beta = 0,\ 0.2,\ 0.4$ and 0.6 GeV. We take the maximum value of β=0.6 GeV and use it for our further considerations.

III. INCLUSIVE PRODUCTION CROSS SECTION

We have employed the idea of factorization to evaluate the J/ψ production cross section at hadron colliders. For $\bar{p}p$ collisions we may write

$$\frac{d\sigma}{dp_T}(\bar{p}p \to c \to J/\psi(p_T)X) = \sum_{i,j}\int dx_1dx_2dz f_{i/\bar{p}}(x_1,\mu)f_{j/p}(x_2,\mu)$$
$$\times\Big[\hat{\sigma}(ij\to c(p_T/z)X,\mu)D_{c\to J/\psi}(z,\mu,\beta)\Big]. \quad (5)$$

Where $f_{i,j}$ are parton distribution functions with momentum fractions of x_1 and x_2, $\hat{\sigma}$ is the charm quark hard production cross section and $D(z,\mu,\beta)$ represents the fragmentation of the produced heavy quark into $\bar{c}c$ state with confinement parameter β at the scale μ. We have used the parameterization due to Martin-Roberts-Stiriling (MRS) [8] for parton distribution functions and have included the heavy quark production cross section up to the order of α_s^3 [9]. The dependence on μ is estimated by choosing the transverse mass of the heavy quark as our central choice of scale defined by

$$\mu_R = \sqrt{{p_T}^2(\text{parton})+{m_c}^2}, \quad (6)$$

and vary it appropriate to the fragmentation scale of the particle state to be considered. This choice of scale, which is of the order of p_T (parton), avoids the large logarithms in the process of the form $\ln(m_Q/\mu)$

or $\ln(p_T/\mu)$. However, we have to sum up the logarithms of order of μ_R/m_Q in the fragmentation functions. But this can be implemented by evolving them by the Altarelli-Parisi equation [10]. The following form of this equation is used here

$$\mu\frac{\partial}{\partial\mu}D_{c\to J/\psi}(z,\mu,\beta)=\int_z^1\frac{dy}{y}P_{Q\to Q}(z/y,\mu)D_{c\to J/\psi}(y,\mu,\beta). \tag{7}$$

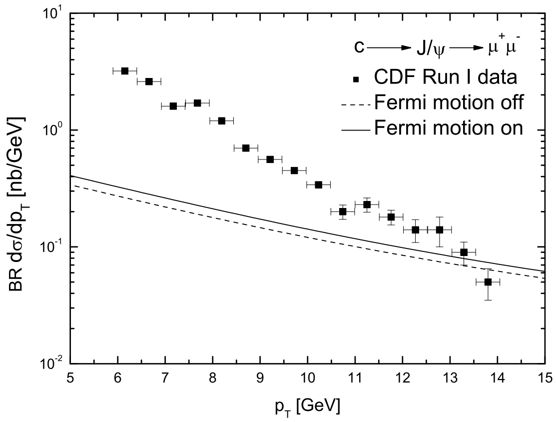

FIG. 2: The differential cross section for direct fragmentation production of J/ψ and its subsequent decay $J/\psi\to\mu^+\mu^-$ at the Tevatron Run I energies. While the dashed curve is obtained using (1) or equally (3) with $\beta=0$, the solid one is due to (3) with $\beta=0.6$ GeV. The result is compared with the CDF Run I data. Other contributions are not included. The scale is chosen to be $2\mu_R$.

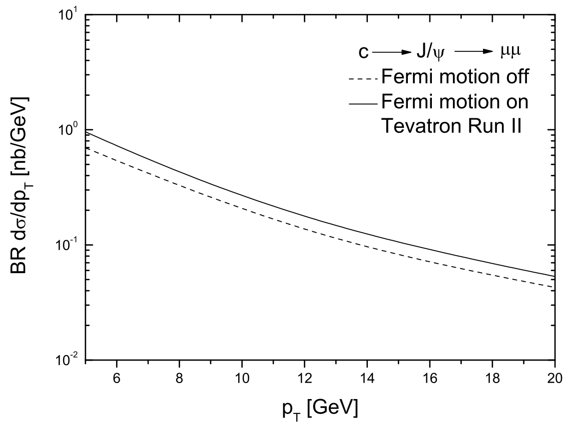

FIG. 3: The differential cross section for direct fragmentation production of J/ψ at Tevatron Run II. The two curves are obtained using (3) with $\beta=0$ and 0.6 GeV respectively. The scale has been set to $2\mu_R$.

Here $P_{Q\to Q}(x=z/y,\mu)$ is the Altarelli-Parisi splitting function. The boundary condition on the evolution equation (7) is the initial fragmentation function $D_{c\to J/\psi}(z,\mu,\beta)$ at some scale $\mu=\mu_\circ$. In principle this function may be calculated perturbatively as a series in α_s at this scale.

Detection of final state requires kinematical cuts of the transverse momentum, p_T, and the rapidity, y. We have imposed the required $p_T^{\rm cut}$ and $y^{\rm cut}$ in our simulations for different colliders as required and have used the following definition of rapidity $y=\frac{1}{2}\log[(E-p_L)/(E+p_L)]$.

IV. RESULTS AND DISCUSSION

In this work we have employed a light-cone wave function to introduce the Fermi motion in J/ψ production in direct fragmentation channel and obtained its fragmentation function in leading order perturbative regime. The behavior of J/ψ fragmentation function with such a wave function is illustrated in Fig. 1.

We have studied the production rates at which the J/ψ state is produced with and without the effect of Fermi motion. First we present the p_T distribution of $\mathrm{BR}(J/\psi\to\mu^+\mu^-)d\sigma/dp_T$ for the cases of the Fermi motion off and on along with the CDF data at Run I in the Fig. 2. The branching ratio $\mathrm{BR}(J/\psi\to\mu^+\mu^-)$=0.0597 is taken from [11]. The poor agreement with data is due to the fact that here we have only considered the contribution of $\bar{p}p\to c\to J/\psi\to\mu^+\mu^-$. Similar behavior at Tevatron Run II energies is shown in Fig. 3. We have also extended our study to the cases of the RHIC and the CERN LHC pp colliders. Here we provide the p_T distributions of the differential cross sections for $c\to J/\psi$ and compare the two cases of the Fermi motion off and on in the Fig. 4. In all cases we have used $\beta=0.6$ GeV for the confinement parameter in

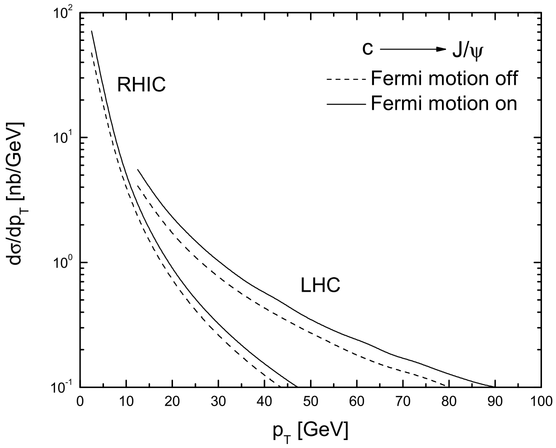

FIG. 4: The differential cross section for direct fragmentation production of J/ψ at the RHIC and the CERN LHC. The shift due to the Fermi motion is significantly increased in the case of LHC but shows to be less important at the RHIC. In both cases the fragmentation function (3) is employed with $\beta = 0$ and 0.6 GeV respectively.

the fragmentation functions. Naturally, the results for β in the range of 0 - 0.6 GeV fall between the above results.

Calculation of the total integrated cross sections for each case shows that the total cross sections for with and without Fermi motion essentially remain unchanged within the uncertainties of Mote Carlo simulations. The reason is first due to the momentum sum rule which the fragmentation functions should satisfy. In other words although the modification of fragmentation functions by the Fermi motion redistributes the final states, the integrated cross sections are left unchanged. Alternatively although the Fermi motion increases the fragmentation probability for the state, i.e., introduces a state with overall higher mass, the cross section is lowered by just the same amount when we introduce the effect in calculation of the total integrated cross section. It is evident from the Figures 2,3 and 4 that the effect increases with increasing $\sqrt{s}$. The kinematical cuts play important role apart from $\sqrt{s}$. The large cross section at the RHIC compared with the LHC in the Fig. 4 is an example.

There are two main sources of uncertainities.The first is about the simulation of J/ψ production at hadron colliders such as the uncertainties along with the fragmentation functions and parton distribution functions. These kind of uncertainties are well discussed in the literature. The second source of uncertainty is due to the choice of the confinement parameter in the fragmentation function. Relying on our discussion in section 2, our choice of $\beta = 0.6$ GeV seems to be justified. Future determination of this parameter will shed more light on this situation. It is worth mentioning that our choice of charm quark mass, i.e., 1.25 GeV, have put our results in their upper side and that the change of the charm quark mass in its acceptable range does not have significant impact on the Fermi motion effect in J/ψ production.

More detailed information concerning this work appears in [12].

[1] E.L. Berger and D. Jones, Phys. Rev. D23 (1981) 1521; R. Baier and R. Ruckl, Z. Phys. C29 (1983) 251.
[2] S.D. Ellis, M. Einhorn and C. Quigg, Phys. Rev. Lett. 36 (1976) 1263.
[3] M. Cacciari and M. Greco, Phys. Rev. Lett. (1994) 1586; K. Sridhar, A.D. Martin and W.J. Stirling, phys. lett. B 438 (1998) 211; A. Petrell, Nucl. phys. Proc. Supp. 86 (2000) 533. Fred Cooper, et al., arXiv:hep-ph/0402219 v2 (2004)
[4] C. Albajar, et al., phys. lett. B256 (1991) 112; F. Abe, et al., Phys. Rev. Lett. 69 (1992) 3704; F. Abe, et al., Phys. Rev. Lett. 71 (1993) 2537; Raphael Granier de Cassagnac, the PHENIX Collaboration, J. Phys. G: Nucl. and Part. Phys. 30 (2004) S1341; D. Acosta, et al., Phys. Rev. D71 (2005) 032001.
[5] G.T. Bodwin, E. Braaten and G. P. Lepage, Phys. Rev. D51 (1995) 1125; E. Braaten, M.A. Doncheski, S. Fleming and M. Mangano, phys. lett. B333 (1994) 548; G.T. Bodwin, E. Braaten and G.P. Lepage, Phys. Rev. D46 (1992) R1914; M. Cacciari and M. Greco, Phys. Rev. Lett. 73 (1994) 1586.
[6] V.A. Khoze, A.D. Martin, M.G. Ryskin and W.J. Stirling, arXiv:hep-ph/0410020 (2004).
[7] M.A. Gomshi Nobary and B. Jvadi, Eur. Phys. J. C. 42 (2005) 37; See also arXiv:hep-ph 0504098 v3 12 Jun 2006.
[8] A.D. Martin, R.G. Roberts and W.J. Stiriling, Phys. Rev. D50 (1994) 6734.
[9] P. Nason, S. Dawson and R.K. Ellis, Nucl. Phys. B303 (1988) 607; W. Beenakker, H. Kuijf, W.L. Van Neerven and J. Smith, Phys. Rev. D40 (1989) 54; W. Beenakker, W.L. Van Neerven, R. Meng, G. Schuler and J. Smith, Nucl. Phys. B351 (1991) 507.
[10] G. Altarelli and G. Parisi, Nucl. Phys. B126, (1977) 298.
[11] Particle Data Group, Phys. Rev. D45 S1 (1992) p. II.18.
[12] M.A. Gomshi Nobary and B. Nikoobakht, Phys. Lett. B639 (2006) 488; hep-ph/0508158.